

Contribution to the Slagging of MgO in Secondary Metallurgical Slags

C. Brüggmann



MgO is an indispensable refractory for modern secondary steel-making. Although its wear behaviour is generally influenced by multiple factors great attention should be paid to chemical wear especially by process slags. So within the scope of this paper aspects of the MgO saturation in secondary metallurgical slags and the corrosion process are taken up. Regarding the chemical wear behaviour the concentration difference of the wear determining component in the slag is of prime importance. Yet inside the slag infiltrated microstructure, subsequently underlying MgO saturation, the corrosion process does never come to rest. In the infiltrated layer of the refractory the mechanisms of particle disintegration and Ostwald-ripening effectively degrade the microstructure giving rise to an erosive wear in practice.

1 Introduction

Nowadays secondary metallurgy provides for the production of steels with highest quality requirements at highest economic efficiency. As an inherent consequence of secondary metallurgical batch processing the refractory lining particularly in a ladle is subject to several severe stresses and thus to a substantial wear. This is underlined by the fact that the ladle lining generates 25–50 % of the whole refractory consumption in steel mills. Especially the slag zone, where according to the state of the art carbonbonded magnesia-carbon (MgO-C) bricks are employed, is

prone to an extreme wear limiting the life cycle of the whole ladle lining. Here the thermo-chemical disequilibrium between process slag and the oxide component of the refractory represents the chief cause. In order to minimize wear and accordingly enhance the lining life cycle the addition of magnesia or magnesia bearing compounds to the process slag, resulting in an early MgO saturation, is (or at least should be) common practice. In literature remarkable increases/decreases are reported for lining life cycle/wear rates in case of marginally considered changes in MgO concentration [2–5].

Consequently the knowledge of MgO saturation dependent on the slag composition and its temperature is of fundamental interest for a smooth, cost-efficient and more environmentally sound steel making. This aspect is dealt with shortly in the second section. In order to optimise and improve

refractories an in-depth understanding of slag corrosion and the underlying mechanisms involved is necessary. Therefore, in the third section aspects of slag corrosion using the practical example of decarburized MgO-C refractory and lime-aluminate slag are briefly summarized and discussed.

A special form of slag corrosion, namely Marangoni-convection at the three phase line MgO – lime-aluminate slag – air, is curtly addressed in the fourth section. Thereby emphasis is put on the effect of the mechanisms pointed out in the third section.

2 MgO saturation

Secondary metallurgical slags are basically described by the quaternary system $\text{Al}_2\text{O}_3\text{--CaO--MgO--SiO}_2$ and may further on be divided into lime-aluminate (Al-killed) and lime-silicate (Si-killed) slags. At a given temperature the chemical wear due to the slag-refractory interaction is strongly dependent on the concentration difference ΔC , i.e. the difference between the saturation concentration and the actual concentration of MgO in the slag. In literature [6–8] aspects of MgO saturation and the interrelationships involved are well summarized. However insufficient consideration is so far given to the following aspects:

- The influence of the $\text{Al}_2\text{O}_3 : \text{SiO}_2$ ratio, i.e. the slag structure at constant basicity on the MgO saturation.
- The double saturation of the slags with MgO and CaO or $2 \text{CaO} \cdot \text{SiO}_2$ (C_2S).
- The temperature dependency, as the previously applied reference temperature of 1600 °C must be increased nowadays to at least 1700 °C.

As the empirical determination of slag equilibria is very time-consuming and expensive,

Christian Brüggmann
ThyssenKrupp Nirosta (since 01.10.2011)
47798 Krefeld
Germany

E-mail: cbrueggmann@yahoo.de

Keywords: ladle slag, MgO saturation, wear and corrosion of MgO refractories

Received: 03.11.2011

Accepted: 15.11.2011

Note

This paper supplements a lecture held on the 8th of September 2010 at the 53rd International Colloquium on Refractories in Aachen / DE in conjunction with the Gustav Eirich Award (3rd Prize) and summarizes the basic impacts of the author's PhD thesis [1] submitted to the Technische Universität Bergakademie Freiberg

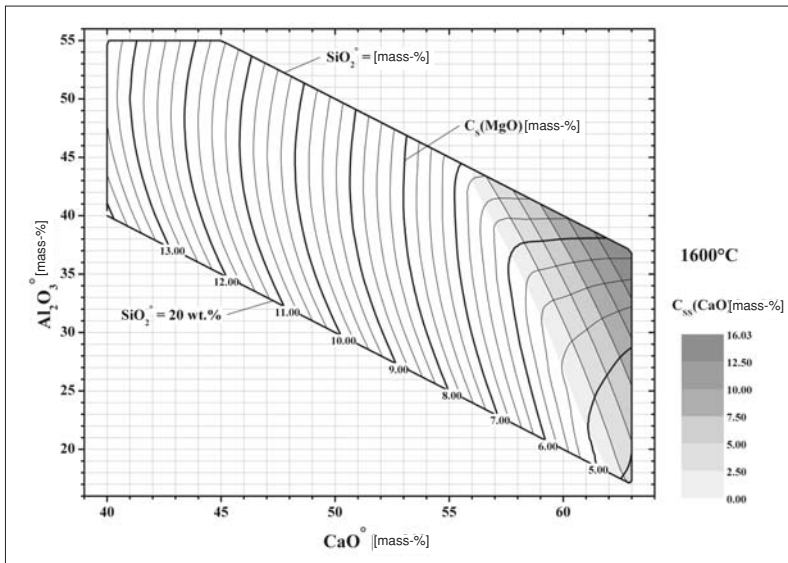


Fig. 1 $C_S(\text{MgO})$ at 1600 °C for lime-aluminate slag, grey-staged shading = range of MgO/CaO saturation [1, 11]

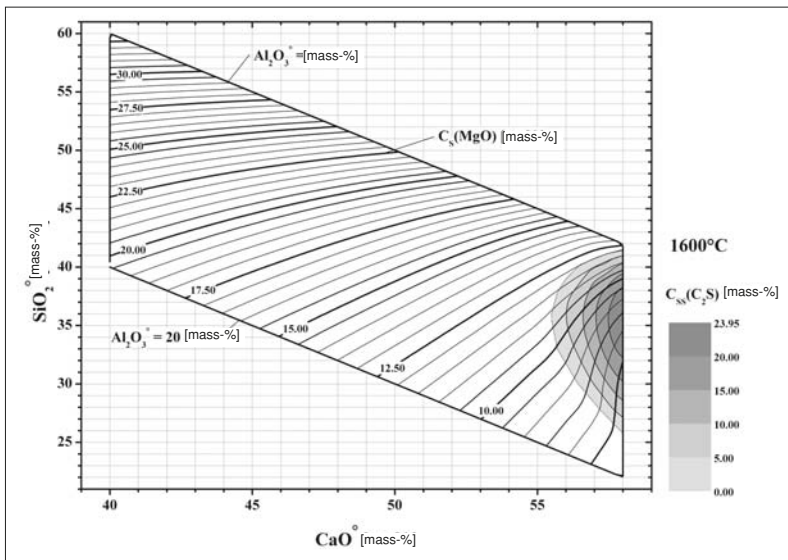


Fig. 2 $C_S(\text{MgO})$ at 1600 °C for lime-silicate slag, grey-staged shading = range of MgO/ C_2S saturation [1, 11]

a convenient alternative exists in the deployment of commercially available thermochemical database and calculation software. In the following, FactSage6.0/Equilib [9] is used to calculate the MgO saturation. Tramp components of the slag such as FeO, MnO and others are neglected on account of their usually low concentration. The slag composition to be equilibrated with MgO is thus reduced to the ternary system of $\text{Al}_2\text{O}_3\text{-CaO-SiO}_2$. This in turn is normalized to 100 mass-% and varied in increments of 1 mass-% within the given limits:

- for lime-aluminate slag:
 $\text{CaO}^\circ = 40 - 63 \text{ mass-\%}$

- for lime-silicate slag:
 $\text{CaO}^\circ = 40 - 58 \text{ mass-\%}$
 $\text{SiO}_2^\circ = 22 - 60 \text{ mass-\%}$
 $\text{Al}_2\text{O}_3^\circ = 0 - 20 \text{ mass-\%}$

An easy-to-read and manageable graphic presentation of the calculated MgO saturation values is then generated with the data analysis and plotting software OriginPro 8G [10] in the form of a x-y-z diagram as a planar contour plot. Figs. 1 and 2 exemplarily show the results of MgO saturation calculation for lime-aluminate and lime-silicate slag at 1600 °C. For presentation of the re-

sults for 1650 °C and 1700 °C see references [1, 11].

From the read-off MgO saturation $C_S(\text{MgO})$ the soluble quantity of MgO $m_{\text{MgO-S}}$ in the normalized slag quantity m_{S-N} is calculated as follows:

$$m_{\text{MgO-S}} = \frac{m_{S-N} \cdot C_S(\text{MgO})}{100 - C_S(\text{MgO})} \text{ [g] or [kg]} \quad (1a)$$

with

$$m_{S-N} = m_{\text{CaO}^\circ} + m_{\text{Al}_2\text{O}_3^\circ} + m_{\text{SiO}_2^\circ} \text{ [g] or [kg]} \quad (1b)$$

Through the worked out diagrams an optimisation in regard to refractory life cycle on the basis of a modified slagging practice (MgO addition, batch calculation) becomes possible. Beyond that a more quantitative interpretation of corrosion experiments undertaken in a lab environment can be conducted.

3 Slag corrosion

From a kinetic viewpoint the slag-refractory-interaction is commonly described with the Nerst equation of boundary layer diffusion:

$$j = \frac{D}{\delta_N} \cdot A \cdot (C_S - C) \text{ [g/s]} \quad (2)$$

j [g/s] is the mass flux, D [cm^2/s] the diffusion coefficient, δ_N [cm] the Nerst boundary layer, A [cm^2] the surface area and $(C_S - C) = \Delta C$ [g/cm^3] the concentration difference or driving force respectively. Considering (2) the mass transport j and inherently the corrosion process comes to rest if $\Delta C = C_S - C = 0$. The slag-refractory system is regarded to be in equilibrium.

However, for dispersed-structured, to some extent consolidated and porous MgO refractories in contact with lime-aluminate or lime-silicate steelmaking slag this commonly accepted conception is only restrictedly applicable.

To underline this thesis Fig. 3 accordingly depicts the results of thermo-gravimetrically followed immersion tests at 1600 °C. Here a fully decarburized MgO-C-cylinder (height: 25 mm, diameter: 18 mm, density: $\rho_R = 2,79 \text{ g}/\text{cm}^3$, porosity $\epsilon = 0,198$, mass $m = 17,7 \text{ g}$, purity MgO > 97 mass-%) is brought in contact with

- a) MgO unsaturated lime-aluminate slag (50 mass-% CaO, 35 mass-% Al_2O_3 , 15 mass-% SiO_2 , $m_{S-N} = 350 \text{ g}$, $m_{\text{MgO-S}} = 37,2 \text{ g}$, see also Fig. 1),

b) MgO saturated lime-aluminate slag (45,2 mass-% CaO, 31,6 mass-% Al₂O₃, 13,6 mass-% SiO₂, 9,6 mass-% MgO, m_s = 387,2 g) in a PtRh 80/20 crucible (inner diameter: 68 mm, inner height: 80 mm). Heating is conducted with 2,5 K/min to 1650 °C with 3 h dwell upon cooling with 2,5 K/min to final temperature of 1600 °C. After 30 min of dwell immersion and measurement is started.

As expected in case b), after a quick infiltration no mass change occurs for quite some time which validates the above calculation of MgO saturation. However, after an immersion time of 91 min the specimen suddenly detaches from its platinum holder. To interpret this remarkable behaviour microstructure analysis with SEM on slag infiltrated and specifically aged refractory specimens is conducted. Fig. 4 shows backscatter electron images of the obtained microstructures after elapsed times of 1, 24 and 48 h with each 300-fold magnification. The solely thermally aged specimen (A, heating with 2,5 K/min to 1650 °C and holding for 3 h upon cooling) shows finely developed sinter necks. The fine aggregates are in their originally ruptured shape which is characterized by spiky corners and defined edges of the particle contour.

Although the slag is saturated with MgO a drastic alteration of microstructure sets in. With accumulating time (specimen pre-treatment as A, B = 1 h, C = 24 h, D = 48 h exposed to MgO saturated slag at 1600 °C) rounded-off, partially almost spherical particles develop which exist in an isolated state, i.e. without frame-forming sinter necks. The resulting microstructures are to be ascribed to two superimposing mechanisms which are known from in the common sense "beneficial" liquid phase sintering and whose common momentum is the minimisation of the total interfacial energy [12, 13]:

Firstly particle disintegration with the following interfacial energy relation

$$\sigma_{MgO} > 2 \cdot \sigma_{slag-MgO} \quad (3)$$

implying that the surface energy of solid-solid-grain boundary σ_{MgO} is larger than twice the interfacial energy of solid-liquid $2 \cdot \sigma_{slag-MgO}$ upon wetting. Given this condition it results that in equilibrium MgO par-

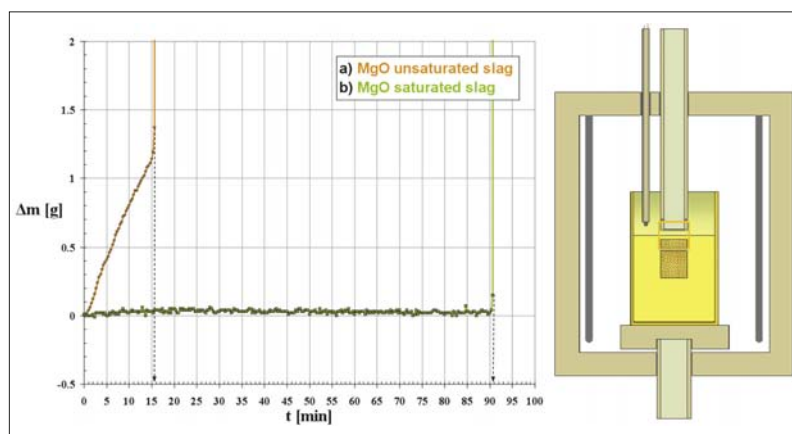


Fig. 3 Time dependent mass change Δm (left) and schematic experimental setup (right)

ticles so to say "float" separately from each other in the slag infiltrated microstructure (compare Fig. 4 B to D).

Secondly dissolution and reprecipitation, summarized as microstructure coarsening, by Gibbs-Thomson-effect or so called Ostwald-ripening given with the following equation

$$c(r) = c_s \cdot \left(1 + \frac{2 \cdot \sigma_{slag-MgO} \cdot V_{MgO}}{r \cdot R \cdot T} \right) \quad [\text{mol/m}^3] \quad (4)$$

$c(r)$ [mol/m³] corresponds to the setting saturation concentration of a convex shaped surface (MgO particle). c_s [mol/m³] accordingly corresponds to the setting saturation

concentration of an infinite flat MgO surface. V_{MgO} [m³/mol] is the molar volume of MgO at 1600 °C, r [m] the particle radius, R [J/(mol · K)] the universal gas constant and T [K] the absolute temperature.

As to be seen from (4) the condition $r < \infty$ is always fulfilled and it follows that $c(r) > c_s$. Thus small and strongly convex shaped surfaces such as particles, particle corners and edges are dissolved. The released concentration of MgO is reprecipitated on less convex shaped surfaces, i.e. customarily larger particles. As a consequence the microstructure coarsens and according to the crystallographic orientation of the cubic MgO energy

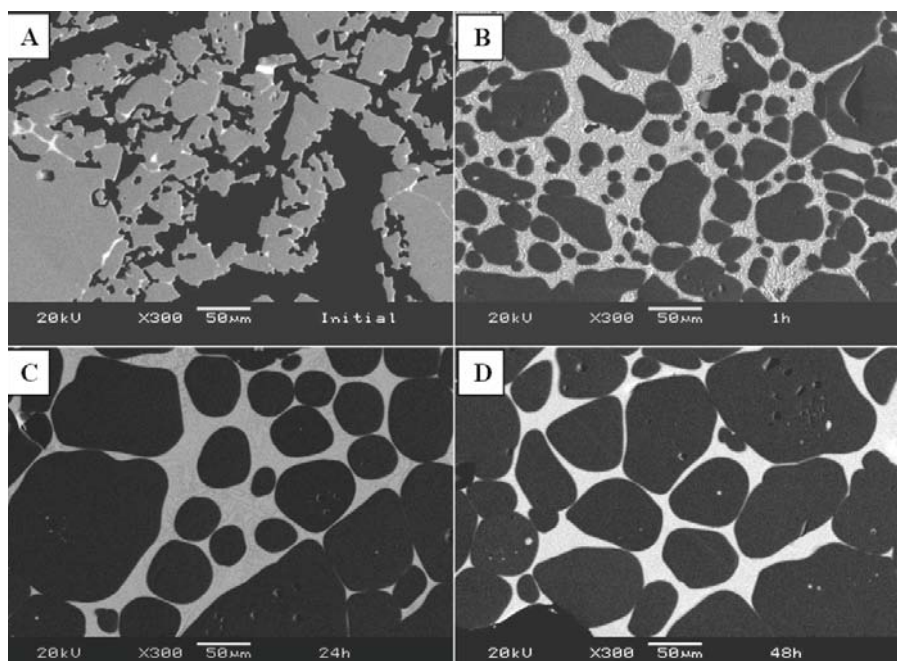


Fig. 4 Backscatter electron images of microstructural transformation of MgO through particle disintegration and Ostwald-ripening, A = 3 h at 1650 °C, no slag = pre-treatment for B, C, D, B = 1 h / C = 24 h / D = 48 h in contact with MgO saturated slag at 1600 °C, 300-fold magnification

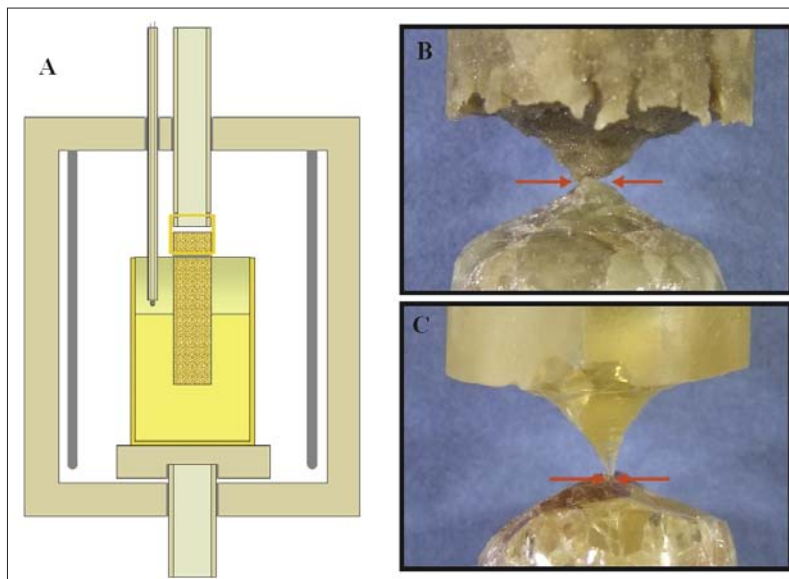


Fig. 5 Schematic experimental setup (A) and macroscopic appearance of specimens after the test at the three phase line, B = sintered MgO ($\epsilon = 0,133$), C = fused MgO ($\epsilon = 0$)

minimized, rounded off particle shapes result (compare Fig. 4 B to C).

Moreover, for very long time all particles of the microstructure pass by except for one single crystal in its equilibrium shape.

In case a), after quick infiltration an almost linear mass change occurs until an immersion time of 16 min. This corresponds to a disaggregation from the surface layer, i.e. the detachment of MgO particles from the surface with a constant rate and further diffusion-determined dissolution in the slag. Thereafter the specimen suddenly degraded completely which corresponds to a homo-

genous disaggregation. Causal is that at first the frame-forming ceramic bonds are weakened by the infiltrating, MgO unsaturated slag. The slag thus becomes saturated. Then in the further course the above mentioned mechanisms determine the moment of homogenous disaggregation.

In both cases the exhibited behaviour is by far more complex. A more quantitative description (modelling) will be published in the near future. Yet, having taken in those aspects, it becomes evident that even with MgO saturation of the slag the microstructure is effectively degraded. It can be stated

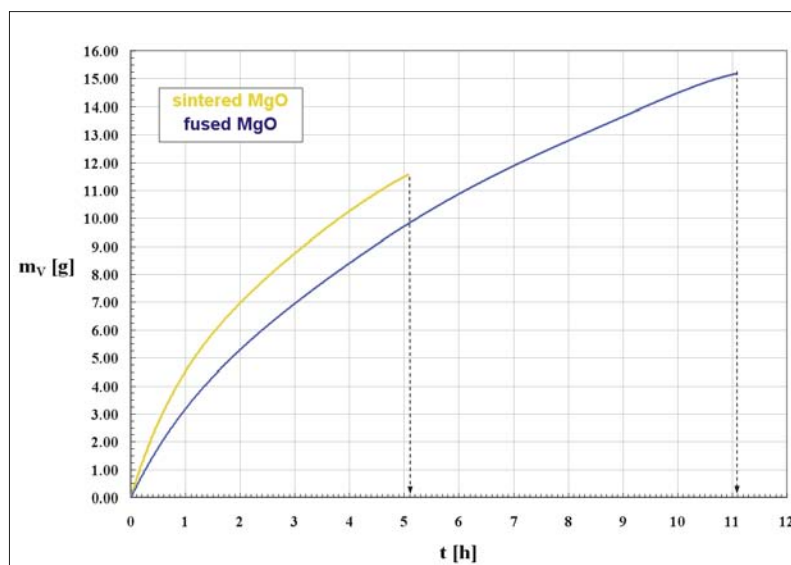


Fig. 6 Time dependent development of actual slagged mass m_v with indication of the moment of cut through

that the corrosion process does never come to rest. In the experiments conducted the slag can be regarded stagnant. In practice (agitated slag due to gas stirring or *Marangoni* convection) it is easily to imagine that the refractory surface layer becomes susceptible to an erosive wear whereat isolated MgO particles or -aggregates are steadily washed away.

4 Marangoni convection

The premature wear of refractories at the three phase line (solid-liquid-gas and solid-liquid-liquid) is to be lead back to the hydrodynamic phenomenon of interfacial or so called Marangoni convection. At the three phase line both heat transfer induced temperature differences (heat dissipation across the refractory lining) and mass transfer induced concentration differences (dissolution and diffusion due to thermo-chemical disequilibrium) cause a gradient of the surface or interfacial tension respectively of the liquid phase [14–16]. This driving force results in a flow which is directed towards higher surface or interfacial tension respectively. Regardless of the flow direction the refractory is directly attacked and dissolved at the Nernst boundary layer. As a consequence the mass transfer is drastically increased so that the magnitude of wear (locally fixed, but advanced corrosion groove) surmounts by far that of diffusion determined dissolution or natural, density driven convection [17].

Embracing the mechanisms pointed out in the third section the effect of microstructure on the so called Marangoni convection is examined by means of thermo gravimetrically followed immersion tests at 1650 °C (see Fig. 5A). Since decarburized MgO-C is gone quickly in unsaturated slag (compare Fig. 3) a cylindrical specimen (height: 55 to 60 mm, diameter: 18 mm) taken from a pressed and sintered MgO brick (density $\rho_R = 3,07 \text{ g/cm}^3$, porosity $\epsilon = 0,133$) is employed and compared with one taken from a lump of fused MgO (density $\rho_R = 3,58 \text{ g/cm}^3$, porosity $\epsilon = 0$). The crystal size amounts up to 9 mm in diameter and several centimeters in length. The slag composition and quantity is analogous to the unsaturated slag described in the third section (see section 3a). Heating is conducted with 2,5 K/min to 1650 °C with 3 h dwell upon immersion and start of measurement. The experiment is finished when the cylinder

is cut through by premature wear due to Marangoni convection.

There to Fig. 5 B and C show the macroscopic appearance at the three phase line after the test. Fig. 6 accordingly gives account on time dependent development of the actual slagged mass m_v which is won by a special calculation routine to be published soon together with model of Marangoni convection. As to be seen fused MgO is cut through after 11 h, pressed and sintered MgO around twice as fast after 5 h. In case of pressed and sintered MgO the shape of the corrosion groove is jagged whilst in case of fused MgO the shape is smooth. Furthermore the cut through happens to be before complete corrosion by Marangoni convection in case of pressed and sintered MgO as indicated by the red arrows. The bearing bond in form of solid-solid bridges or sinter necks respectively is virtually gone earlier. In comparison fused MgO wears up to a shape with a needle like tip.

From the backscattered electron images of the bottom part of pressed and sintered MgO (see Fig. 7) it becomes clear that the mechanisms of particle disintegration and Ostwald-ripening substantially interfere with Marangoni-convection as well. The left image shows the immediate detachment of a crystallite from the bulk (sintered coarse grain) at the phase boundary. The right image erosively detached, down-dwindling and rounded off crystallites in front of the actual phase boundary.

5 Conclusion

Regarding lining life cycle from a metallurgical viewpoint diligence is to be paid to the slagging practice. From a material science viewpoint the question comes up how to counteract or delay the destruction of the ceramic bonds by slag within the scope of the practical requirements. Without controversy this has solely to be realized by an accordingly built surface energy minimized, yet porous ceramic microstructure. Thus in further works the influencing factors of the disperse state, the shaping as well as the pre-treatment or finishing should be regarded and examined carefully for their efficiency. Hereunto this work represents, due to its quantitative treatment and its subsequent drawn results, a contribution to the specific examination of corrosion processes and could therefore find its way into future laboratory praxis.

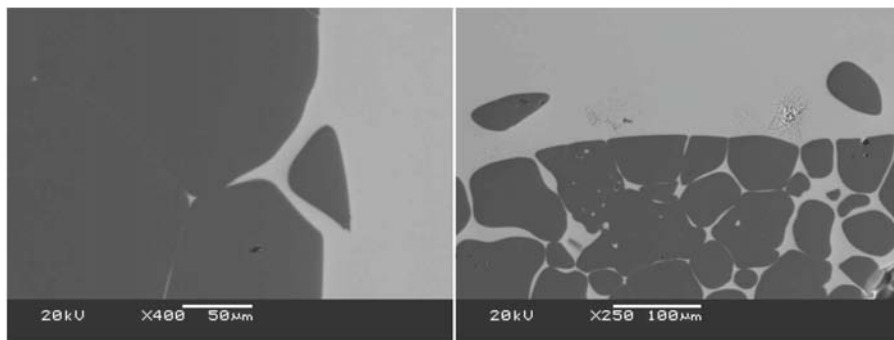


Fig. 7 Backscatter electron images at the phase boundary of the bottom part of sintered MgO

6 Acknowledgement

I want to express my exceptional and sincere gratitude to *Prof. Dr.-Ing. habil. J. Pötschke* (Essen/DE) for his steady interest in the progress of this work and the numerous, valuable suggestions and lively discussions. As well I am very much indebted to *Prof. Dr.-Ing. habil. C.G. Aneziris* (Professorship of Ceramics at the *Institute of Ceramics, Glass and Construction Materials* at the *TU Bergakademie Freiberg/DE*) for the open and fruitful discussion and his steady support in academic questions.

Words of thank also go to *Prof. Dr. rer. nat. P. Quirnbach* (managing director of the *Forschungsgemeinschaft Feuerfest e.V.*, Bonn/DE) for supporting my work during the course of daily affairs and for encouraging me to participate in the Gustav Eirich Award 2010.

7 References

- [1] Brüggmann, C.: Ein Beitrag zur Verschlackung von MgO in sekundärmetallurgischen Schlacken. Submitted PhD thesis, TU Bergakademie Freiberg, 27.09.2010
- [2] Erny, E.L.: Refractory wear of magnesia-carbon brick in ladle furnace (LF) slaglines. Proc. 11th UNITECR, 13–16 October 2009, Salvador, Brazil
- [3] Wöhrmeyer, C.; Jolly, R.; Brüggmann, C.: Novel fluxing agent for slags in secondary steel ladles to improve refractory life time and steel quality. 26. celostátní konference se zahraniční účastí: Teorie a praxe výroby a zpracování oceli, 14–15 April 2010, Roznov pod Radhostem, Czech Republic, p. 72–76
- [4] Wöhrmeyer, C.; Elorza-Ricart, E.; Jolly, R.; Guichard, S.; Brüggmann, C.; Sax, A.: The impact of synthetic slags on steel ladle refractory life time. Proc. 51st Internat. Colloquium on Refractories, 15–16 October 2008, Aachen, Germany, p. 80–83
- [5] Reisinger, P.; Presslinger, H.; Hiebler, H.; Zednick, W.: MgO-Löslichkeit in Stahlwerksschlacken. BHM Berg- und Hüttenmännische Monatshefte 144 (1999) [5] 196–203
- [6] Koch, K.; Trömel, G.; Heinz, G.: Das Hochofenschlackensystem Al_2O_3 -CaO-MgO-SiO₂ bei 1600, 1500 und 1400 °C. Archiv für das Eisenhüttenwesen 46 (1975) [3] 165–171
- [7] Bergmann, B.; Bannenber, N.: Schlackenführung und Schlackenoptimierung in der Sekundärmetallurgie. Stahl und Eisen 111 (1991) [1] 125–131
- [8] Park, J.M.; Lee, K.K.: Reaction equilibria between liquid iron and $CaO-Al_2O_3-MgO_{sat}-SiO_2-Fe_2O-MnO-P_2O_5$ slag. 79th Steelmaking Conference, Pittsburgh, USA 1996, p. 165–172
- [9] www.factsage.com
- [10] www.originlab.com
- [11] Brüggmann, C.; Pötschke, J.: MgO saturation in secondary metallurgical lime-aluminate and lime-silicate slags. Steel Research International, accepted 26.10.2010, DOI 10.1002. srin. 201000236, in print
- [12] Telle, R.: Sintern, in: Salmang/Scholze Keramik. R. Telle (Ed.), 7th Edition, Springer Berlin, Heidelberg, New York, 2007
- [13] Schatt, W.: Sintervorgänge – Grundlagen. VDI-Verlag GmbH, Düsseldorf 1992
- [14] Hrma, P.: Dissolution of a solid body governed by surface free convection. Chem. Engng. Sci. 25 (1970) 1679–1688
- [15] Mukai, K.: Marangoni flows and corrosion of refractory walls. Philosophical Transactions of the Royal Society of London, The Royal Society, Vol. 365 (1998) p. 1015–1026
- [16] Brückner, R.: Die zu Erosionen an Modellsubstanzen und feuerfesten Stoffen führenden Grundmechanismen der Grenzflächenkonvektion. Glastechn. Ber. 40 (1967) [12] 451–462
- [17] Hauck, F.G., Pötschke, J.: Der Verschleiß von Tauchausgüssen beim Stranggießen von Stahl. Archiv für das Eisenhüttenwesen 53 (1982) [4] 133–138